Global analysis of radiative forcing from fire-induced shortwave albedo change

G. López-Saldaña[1], I. Bistinas[1] and J.M.C. Pereira[1]

[1]{ Centro de Estudos Florestais, Instituto de Agronomia, Universidade de Lisboa, Tapada da Ajuda, 1349-017 Lisboa, Portugal }

Correspondence to: G. López-Saldaña (GerardoLopez@isa.utl.pt)

Abstract

Land surface albedo, a key parameter to derive Earth's surface energy balance, is used in the parameterization of numerical weather prediction, climate monitoring and climate change impact assessments. Changes in albedo due to fire have not been fully investigated at continental and global scale. The main goal of this study therefore, is to quantify the changes in instantaneous shortwave albedo produced by biomass burning activities and their associated radiative forcing. ~~The main goal of this study therefore, is to quantify the changes in albedo produced by biomass burning activities and their associated shortwave radiative forcing.~~

The study relies on the Moderate Resolution Imaging Spectroradiometer (MODIS) MCD64A1 burned area product to create an annual composite of areas affected by fire and the MCD43C2 BRDF-Albedo snow-free product to compute a bihemispherical reflectance time series. The approximate day of burn is used to calculate the instantaneous change in shortwave Albedo. Using the corresponding National Centers for Environmental Prediction (NCEP) monthly mean downward solar radiation flux at the surface, the global radiative forcing associated to fire was computed.

The analysis reveals a mean decrease in shortwave albedo of –0.01~~423~~ (1σ = 0.01~~78~~) causing a mean positive radiative forcing of ~~6.31~~3.99 Wm^{-2} (1σ = ~~5.04~~4.89) over the 2002 - 20012 time period in areas affected by fire. The greatest drop in mean shortwave albedo change occurs in 2002, which corresponds to the highest total area burnt (3~~.78~~~~66~~ Mha) observed in the same year and produces the highest mean radiative forcing (~~6.75~~4.5 Wm^{-2}).

Africa is the main contributor in terms of burned area but forests globally are giving the highest radiative forcing per unit area, thus give detectable changes in shortwave albedo. The global mean radiative forcing for the whole studied period ~0.02754 Wm^{-2} shows that the contribution of fires into the Earth system is not insignificant.

1 Introduction

Land-surface conditions have a strong impact on the Earth's system energy balance through changes in land surface albedo that induce a radiative forcing by perturbing the shortwave radiation budget (Ramaswamy et al., 2001). The total solar incoming radiation has a mean strength of ~1366 Wm^{-2} ("solar constant") and has an irregular cycle of about 11 years, causing a variation of ±0.5 Wm^{-2} (Gray, 2010). Since, on average, the Earth absorbs energy at the rate of $(1 - A)I_{TS}/4$ (Gray, 2010), where A is the Earth's albedo and I_{TS} the total solar irradiance, taking $I_{TS} = 1366$ Wm^{-2} and a mean albedo of the Earth $A = 0.3$ (Prentice at al., 2012), the solar power available to the whole Earth system is 239.05 Wm^{-2}. The importance of quantifying changes in albedo arises here. The global mean concentration of CO_2 in 2005 was 379 ppm, leading to a radiative forcing of +1.66 Wm^{-2} ($1\sigma = 0.17$). ~~The radiative forcing caused by CO_2 is 1.56 Wm^{-2}~~ (Forster et al., 2007) while that of changing the planetary albedo by as little as 0.01 can produce a change of the radiation balance of 2.39 Wm^{-2}, revealing the role that even small changes in albedo can have a substantial impact in the Earth system.

Fire has a strong influence on climate due to the release of atmospheric aerosols and gases and can modify surface albedo by removal of vegetation and deposition of ash and charcoal (Bowman, 2009). Earlier studies aimed to quantify the impact of fires on the land surface albedo. Govaerts et al. (2002) analysed a Meteosat albedo time series for 1996 in Northern Hemisphere Africa and using fire-induced albedo perturbation probabilities, estimated that fires are responsible for a relative albedo decrease as large as 25 %. Jin and Roy (2005) used MODIS data to estimate a mean 2003 instantaneous shortwave albedo change of −0.024 over all the burned areas in the Australian tropical savana, which exerted a shortwave surface radiative forcing of 6.23 Wm^{-2}. Several studies have been carried out in the boreal area, Jin et al. (2012a) analysed the sensitivity of spring albedo to the MODIS-derived difference Normalized Burn Ratio (dNBR) while Jin et al. (2012b) found a fire-induced surface shortwave forcing (SSF) integrated over an annual cycle of -4.1 Wm^{-2} between southern and northern boreal regions. ~~Earlier studies aimed to quantify the impact of fires on the land~~

~~surface albedo. Govaerts at al. (2002) analysed a Meteosat albedo time series for 1996 in Northern Hemisphere Africa and estimated that fires are responsible for a relative albedo decrease as large as 25%, while Jin and Roy (2005) used MODIS data to estimate a mean 2003 shortwave albedo change of -0.024 over all the burned areas in the Australian tropical savana, which exerted a shortwave surface radiative forcing of 6.23 Wm^{-2}~~. However, studies over longer time periods at global scale are needed to improve the understanding of the influence of fire in the Earth system as an agent of land surface alteration and its impact on the energy balance.

No earlier studies have attempted to quantify the impact of fire on shortwave albedo at global scale; therefore, the main goal of this study is to quantify the "instantaneous" shortwave albedo change in areas affected by fire and the corresponding radiative forcing at the surface. The radiative forcing contributed by aerosols produced by fires is not considered, since the scope of the study is to investigate exclusively the impact of fires at the surface. We derived an albedo time series and then calculated the difference in the pre- and post-fire shortwave albedo only in areas affected by fire for the 2002 – 2012 time period. The radiative forcing exerted by the changes in albedo was calculated using the total solar incoming radiation.

2 Data

2.1 Albedo time series generation and burned area identification

The shortwave albedo time series was generated using the MODerate-resolution Imaging Spectroradiometer (MODIS) Collection 5 BRDF/Albedo snow-free quality product (MCD43C2) (Schaaf et al., 2002). It is produced on a 16-day basis with an 8-day overlap projected to a 0.05º latitude/longitude Climate Modelling Grid (CMG). The product models the surface anisotropy using all high quality, cloud-free, snow-free and atmospherically corrected land surface reflectance obtained within a 16-day time period. When there are more than seven of these observations, a so-called *full model* inversion is attempted to retrieve the BRDF parameters based on the RossThickLiSparse-Reciprocal Bidirectional Distribution Reflectance (BRDF) model (Lucht et al., 2000). If there are only 3 to 6 of the aforementioned observations over the 16-dat time period, a backup algorithm is used, it is based on a archetypal BRDF model parameters which is defined with respect to 25 global land cover classes and from historical high quality retrievals (Ju et al., 2010). Data for 11 years, 2002 to

2012 was downloaded from the Land Processes Distributes Active Archive Center (LP DAAC) data pool.

In order to use only the highest quality data, the BRDF_Quality science data set provided with the MCD43C2 was analysed. Only pixels with *best quality* (75_% or more with best full inversions) and *good quality* (75_% or more with full inversions) were kept for further processing. The Global bi-hemispherical reflectance (α_{BHR}) under isotropic illumination, also designated white-sky albedo, for every 16-day time period was computed using:~~Using the three BRDF model parameters, the isotropic f_{iso}, volumetric f_{vol} and geometric f_{geo}, from the shortwave broadband (0.3-5.0µm) the global bihemispherical reflectance (BHR) under isotropic illumination named as well as white-sky albedo for every 16-day time period was computed using:~~

$$\alpha_{BHR}(\lambda) = f_{iso}(\lambda)g_{iso} + f_{vol}(\lambda)g_{vol} + f_{geo}(\lambda)g_{geo} \quad (1)$$

where f_{iso}, f_{vol} and f_{geo} are the three BRDF model parameters, isotropic, volumetric and geometric. The integrated coefficients have the following values: $g_{iso} = 1.0$, $g_{vol} = 0.189184$ and $g_{geo} = -1.377622$.~~and the integrated coefficients shown in Table 1.~~

Some areas can show gaps caused by lack of high quality data and by the screening based on the BRDF_Quality flag. A linear temporal interpolation was computed to create a synthetic, temporally and spatially continuous shortwave albedo product. The interpolation was performed on a yearly basis but taking into account one month before and after the calendar year to be able to fill gaps at the very beginning or at the very end of the year. The final product consists of a gap-free 16-day (with an 8-day overlap) snow-free broadband shortwave albedo time series with a 0.05º spatial resolution for 2002 to 2012.

2.2 Burned area identification

The areas affected by fire ~~per~~ each year were derived using the MODIS Collection 5.1 Direct Broadcast Monthly Burned Area Product (MCD64A1) (Gilgio et al., 2009). The product identifies post-fire burned areas using daily 500m surface reflectance coupled with 1km MODIS active fires observations. Twelve years of data were downloaded from (MCD64A1 burned area product) spanning from 2002 to 2012. The spatial resolution of the product is 500m and is generated on a monthly basis. It was necessary to perform a spatial aggregation on the monthly datasets to 0.05º using a mode filter to match the CMG spatial resolution. .

The proportion of the CMG pixel that was affected by fire was calculated, thus giving a fractional burn area estimate. When more than one date was found inside a CMG pixel the mode of the day of burn was set as the day of burned. The annual burned area dataset was generated selecting the approximate day of burned from the monthly datasets. When more than one day was found the earliest date was selected.

2.3 Land Use Land Cover (LULC) maps

The MODIS Collection 5.1 Land Cover Type Yearly (MCD12C1) (Friedl et al., 2010) is produced at 0.05º spatial resolution and provides the dominant land cover type and the sub-grid frequency land cover class distribution within each 0.05º cell.

In order to analyse major biomes an aggregation of the land cover classes was performed. For every year from 2002 to 2012: 1) all forest classes (evergreen needleleaf forest, evergreen broadleaf forest, deciduous needleleaf forest, deciduous broadleaf forest, mixed forests) were aggregated into a single "Forest" class, 2) croplands, cropland/natural vegetation mosaic was aggregated into the "Croplands" class and 3) closed shrubland, open shrublands, woody savannas, savannas, grasslands and permanent wetlands were aggregated into the "non-forest" class. The aggregation takes into account the confidence level, only when confidence was bellow 60 % the "majority land cover type 2" was used.

Additionally to the analysis per land cover, an analysis per continent will be performed. ~~The regions used in the study are depicted in figure 1.~~

2.4 Downward shortwave solar radiation flux at the surface

The National Centers for Environmental Prediction and the National Center for Atmospheric Research (NCEP/NCAR) Reanalysis 1 (Kalnay et al., 1996) provides the monthly mean downward solar radiation flux (dswrf) at the surface in Wm^{-2} at 1.8º by 1.8º grid cells from 1948 to 2013. The full reanalysis dataset was obtained from (NCEP/NCAR dswrf at the surface). A temporal subset was extracted to obtain 12 years of monthly dswrf from 2002 to 2012.

3 Quantification of albedo change and associated radiative forcing

3.1 Method description

For every pixel ~~identify~~ identified as affected by fire within a calendar year, the change in broadband shortwave albedo is calculated as

$$\Delta A_{fire} = A_{post} - A_{pre} \quad (2)$$

where ΔA_{fire} is the "instantaneous" land surface shortwave albedo change when subtracting the pre-fire albedo (A_{pre}) from the post-fire albedo (A_{post}).

The selection of the dates to compute the change in albedo is not straightforward, and several factors must be taken into account.

First, the albedo time series was computed using the BRDF model parameters and these parameters were derived fitting a BRDF model using all high quality observations within a 16-day time period. The assumption is that even when there may be day-to-day changes in land surface condition these high quality observations have normally distributed random noise and can describe the BRDF (Lucht and Lewis, 2000). However, fire affects vegetated areas, which generally are very reflective in the near-infra-red and after a burning event, show a decrease in reflectance due to vegetation loss and deposition of charcoal and ash (Pereira, 1999; Stroppiana, 2002). Additionally some fire events may last more than one day in several areas around the globe (Chuvieco et al., 2008). Therefore the 16-day time periods adjacent to the approximate day of burned might have used mixed observations, burned and non-burned, to fit the BRDF model resulting in a smooth transition from the pre-fire to post-fire albedo rather than a sharp change.

Second, there ~~is~~ are uncertainties ~~uncertainty~~ in the day of burning. The MCD64A1 product relies on both, daily surface reflectance and daily fire masks. However, a minimum of approximately ten days of cloud-free observations before and after to accommodate the moving windows employed in the change-detection process are needed, lack of data due to clouds or coverage gaps double the number of days required (Gilgio et al., 2009). Additionally the Quality Assessment (QA) Scientific Dataset (SDS) masks surface reflectance pixels when an active fire is detected, which increases the temporal uncertainty in the identification of the day of burned.

Given these two factors, an analysis to quantify the length of the window, centred at the approximate day of burn, which is needed to compute the change in albedo was carried out. The result is that a 32-day window is the best to be used at global scale. The A_{pre} date was set identifying the maximum albedo previous to the fire occurrence, while the A_{post} date the minimum albedo value after the fire.

Ramaswamy et al. (2001) define radiative forcing as 'the change in net (down minus up) irradiance (solar plus longwave; in Wm^{-2}). In this study we do not consider longwave forcing. Once the change in albedo ΔA_{fire} was computed, the shortwave radiative forcing at the surface ΔF_0 exerted by changes in shortwave albedo due only to fire is estimated as:~~Ramaswamy et al. (2001) define the radiative forcing as 'the change in net (down minus up) irradiance (solar plus longwave; in Wm^{-2})' and since for this study we neglect any longwave forcing, once the change in albedo ΔA_{fire} was computed, the shortwave radiative forcing at the surface $\Delta F_{surface}$ exerted by changes in shortwave albedo only due to fire is estimated as:~~

$$\Delta F_0 = -dswrf_0^{\downarrow}\, \Delta A_{fire}$$

where $-dswrf_0^{\downarrow}$ is the monthly mean downward solar radiation flux (dswrf) at the surface in Wm^{-2}., the subscript ($_0$) denotes the quantity at the surface.

4 Results

The global spatial distribution of mean radiative forcing caused by "instantaneous" shortwave albedo changes on areas affected by fires is depicted in Fig. 1. Most fires occur in the tropical and sub-tropical environments. High values of radiative forcing, e.g., greater that 5 Wm^{-2} in those areas, shown in dark red tones, might suggest frequent intense fire occurrence like in South Sudan, Angola and Northern Australia, whereas low forcing in dark blue tones, like the big cluster in Ukraine and the South West corner of the Russian Federation are related to frequent non intense fires.

Overall, the trend in burned area for the whole studied period is negative, however the albedo change and the radiative forcing show no significant trend (Fig 2). The mean albedo changes, considering the change between post-fire shortwave albedo minus the pre-fire value, have a slightly annual increase opposite trend of the total annual area burned. ~~Overall, the trend in~~

~~mean annual radiative forcing for the whole studied period is negative, in agreement with the trend of the total annual area burnt (Figure 2). The mean albedo changes, considering the change between post-fire shortwave albedo minus the pre-fire value, have the opposite trend of the total annual area burnt.~~ Fundamentally, a fire event will decrease the shortwave albedo, resulting in a positive radiative forcing in return, Figs. 5 and 6 show for the Sahel and Australia correspondingly: the approximate day of burn (DoB), instantaneous shortwave albedo change, the relative albedo change and the associated radiative forcing. Areas in red tones indicate a large change and areas in blue tones small change in the albedo changes.~~(Figure 5-6)~~. Nevertheless the consistent decrease in burned area did not produce a significant decrease in albedo changes, that could be explain due to alterations in fire intensity.

The global mean change in albedo is –0.014 (σ = 0.017) causing a mean positive radiative forcing of 3.99 Wm^{-2} (σ = 4.89) on a global mean annual burned area of 349.48Mha (σ = 21.81Mha) during the 2002 to 2012 time period.

In order to quantify the global or regional impact, it is necessary to normalize the forcing by the proportion of the total area burned to the total surface. Given r = 6371007.181m as the radius of the idealized sphere representing the Earth; the total global surface is $4\pi r^2$, ~510.07Mkm^2. Assuming a proportion of land in the planet of 30%, given the mean radiative forcing in areas where fire occurred during 2002–2012 is 3.99Wm-2, the global mean forcing only in land is 1.197 Wm^{-2}. The mean annual global area affected by fires during the 11 years comprising the study period is 349.48Mha or 3.4948 Mkm^2, ~0.69 % of the Earth's surface. Using again the mean radiative forcing in areas where fire occurred during 2002–2012, 3.99Wm^{-2}, multiplying by the proportion of area affected by fire, the global mean radiative forcing is 0.0275Wm^{-2}. When performing the same calculation at regional scale, for instance, Australia, the mean radiative forcing is 5.71Wm^{-2}, and the mean area burned is 0.502 Mkm^2, representing the 6.53 % of the Australian territory. Therefore, the mean radiative forcing for Australia is 0.373 Wm^{-2}, an order of magnitude higher than the global number.

4.1 Interannual variability and land cover affected

At the global scale, the highest mean radiative forcing occurs in forested areas, in 2003, in 2006 and in 2010. Croplands and non-forests have a stable inter-annual cycle with the

exception of 20023 and 20043 respectively being the years with the highest mean values (Figure Fig. 4).

The main discrepancies between area burnedt and radiative forcing occur in the period of 2005-2007, where intermediate-high area burnt is associated with the lowest values of radiative forcing in 2005 and 2007, and a high abrupt peak in 2006.

The greatest drop in mean shortwave albedo change occurs in 2002, which corresponds to the highest total area burnedt (3.66 78Mha) observed in the same year and produces the highest mean radiative forcing (4.56.75 Wm^{-2}) (Fig.ure 2). The lowest shortwave albedo change values in 2005 and 2007 areis not associated to low area burnedt and similarly the lowest and very abrupt drop of area burnt in 2009 does not produce the lowest albedo change and radiative forcing (Fig.ure 2).

Most fires occur in the Sahel (FigureFig. 5) and the Australian savanas (FigureFig. 6) corresponding to an average up to 89 % of the total global area burnt, whereas the highest radiative forcing per unit area is located in forests of Australia in 2003 and 2006, Europe in 2010 and Asia in 2002, with mean continental values of 15.43 Wm^{-2}, 15.26 Wm^{-2}, 13.98 Wm^{-2} and 8.81 Wm^{-2} respectively (Fig. 3).whereas the highest radiative forcing per unit area is located in forests of Europe in 2010, Australia in 2003 and 2006 and Asia in 2003, with mean continental values of 27 Wm^{-2}, 20.4 and 21 Wm^{-2}, and 15.3 Wm^{-2} respectively (Figure 3). In croplands, Asia shows the highest radiative forcing and the greatest oscillations with a minimum of 2.116.79 Wm^{-2} in 20045 and maximum of 610.1.8 Wm^{-2} in 20083 (Figure Fig. 3). The rest of the continents show a low variability in cropland areas, with the exception of Australia in 2003 showing a steep peak of 10.56.54 Wm^{-2}. In non-forests, the highest radiative forcing is in North America in 2004, in Europe in 200710 and in Asia in 20023 and 2010. High oscillations are also observed in Australia with an abrupt drop in 2010, contrasting with very stable inter-annual cycle of Africa. Fig. 7 shows the temporal evolution of burned area over Northern Africa and Australia, showing opposite behaviours. Whilst in Northern Africa the tends to decrease and there is not significant trend in the associated radiative forcing, in Australia, the burned area over the 11-year time period shows a positive trend associated to a negative trend in the corresponding radiative forcing, this suggest more areas affected by fire but not necessarily associated to high burned severity.

~~The global mean change in albedo is −0.023 (σ = 0.018) causing a mean positive radiative forcing of 6.31 Wm^{-2} (σ = 5.04) on a global mean annual burned area of 349.48Mha (σ = 21.81Mha) during the 2002 to 2012 time period.~~

~~In order to quantify the global or regional impact, it is necessary to normalize the forcing by the proportion of the total area burned to the total surface. Given r = 6371007.181m as the radius of the idealized sphere representing the Earth; the total global surface is $4\pi r^2$, ~510.07Mkm^2. The mean annual global area affected by fires during the 11 years comprising the study period is 349.48Mha or 3.4948 Mkm^2, ~0.69% of the Earth's surface. Since the mean radiative forcing only in areas where fire occurred during 2002-2012 is 6.31 Wm^{-2}, the global mean radiative forcing is ~0.04 Wm^{-2}. When performing the same calculation at regional scale, for instance, Australia, the mean radiative forcing is ~7.66 Wm^{-2}, and the mean area burned is 0.502 Mkm^2, representing the ~6.53% of the Australian territory leading to a mean radiative forcing for Australia of ~0.49 Wm^{-2}, an order of magnitude higher than the global number.~~

5 Discussion and conclusions

We have presented a study to quantify the temporal evolution of fire-induced albedo changes and the continental and global annual mean forcing estimations. ~~In here,~~ W~~w~~e here used the radiative forcing as a measure to quantify the influence and contribution of fire in the Earth's energy balance, and showed that fired caused a consistent decrease the land surface shortwave albedo, leading to a positive radiative forcing.

5.1 Extreme events

Continental Europe includes Russian territories and, has as eastern borders the Ural mountains, the Ural river and the Caucasus mountains, as well as the water line of Caspian lake. Therefore, the anomalous fire events in July 2010 around Moscow are included in European continent. On an annual basis, in Russia, 90-95 % of burnt areas are located in the Asian part of Russia with the majority (59.3 %) being forests, with the exception of the extreme event of 2010 (Shvidenko et al., 2011). The abrupt peak in 2010 in ~~Figure~~Fig. 3e corresponds to that event exactly with mean annual value for forests in continental Europe of ~~27~~ 13.98Wm^{-2}. The mean continental value is more realistic when compared to the massive

maximum number of 167 Wm^{-2} for the same event including aerosols in smoky conditions found in the literature (Chubarova et al., 2012).

Similar extreme events can be observed in Fig. ~~ure~~ 3f in 2003 and 2006 in Australia, depicting the Eastern Victorian alpine fires, which burnt 1.3 ~~–~~Mha in 2003, and the Grampians in Victoria in 2006 that burned 184 ~~,~~000 ha. A plausible explanation is that a weak to moderate El Niño event had a very strong impact in Australia causing the major 2002-2003 drought had rainfall deficiencies over the period March 2002 to January 2003 (Australian Government, 2014). Fires affected eastern New South Wales (NSW), Canberra, and the mountains areas of southeast NSW and forested areas in eastern Victoria as show in Fig. ~~figure~~ 6 ~~upper-left panel~~. A radiative forcing above 2~~1~~5 ~~–~~Wm^{-2} over northeast Victoria and the Great Dividing Range Mountains in the Kosciuszko National Park in southern NSW mainly to a large shortwave albedo decrease due to forest fires is shown in Fig. ~~figure~~ 6. Broadly, forest has a low shortwave albedo ~0.3 that varies with the viewing and illumination conditions (Liang, 2000). Given the extraordinary circumstances during the 2002-2003 drought in Australia, the forest fires dramatically altered the albedo, up to a 60 % relative change in some areas (Fig. 6), during the Austral summer (pick of incoming radiation), nevertheless changes due to seasonality, e.g., vegetation senescence that affects surface reflectivity were not taking into account and a contribution of the decrease in albedo in the Australian summer might be due to these non-fire related changes.

In ~~Figure~~Fig. 3b, the highest value of radiative forcing occurs in 2003 when the massive boreal fires in western Siberia burning over 20 Mha and being one of the largest forest fires on record (Sheng et al., 2004). Croplands and non-forests are following the west Siberian event of 2003, showing the highest mean radiative forcing value of all cropland areas (Fig. 3b).

In North America in 2004 there is the highest continental value of mean annual radiative forcing occurring in non-forests (~~15.38~~ 9.89Wm^{-2}). The summer of 2004 was an extensive fire season in Alaska and western Canada with the majority of the area burnt happening grasslands (including shrublands) and forests (Turquety et al., 2007).

In South America the three-year intervals of increased radiative forcing might be associated to teleconnections causing extensive droughts like in 2010 (Lewis et al., 2011), that increase fire incidence in forests and savanas, but also to anthropogenic activities (Aragão and Shimabukuro 2010).

5.2 Concluding remarks

Changes in shortwave albedo are not the only source of radiative forcing when fires affect the land surface. According to the Intergovernmental Panel on Climate Change (IPCC) Fourth Assessment Report, biomass burning accounts for the 75% of the direct radiative forcing from organic aerosols and it is estimated at -0.5 ± 0.5 Wm^{-2} for the period of 1750 - 2005 (Forster et al., 2007). In the tropics, where incident solar radiation is larger than at higher latitudes, it can enhance the radiative effect from aerosols (Holben et al., 2001). Ross et al., 1998 found a radiative forcing of about -15 ± 5 Wm^{-2} during the 1995 Amazon fire season. Total black carbon emissions from biomass burning (3.3 TgC yr^{-1}) represent 40% of the total black carbon emissions, with an additional 4.6 TgC yr^{-1} contributed by fossil fuel and biofuel combustion (Bond et al., 2004). Although the overall radiative forcing of smoke aerosol particles is negative, black carbon can produce positive radiative forcing. The global radiative forcing of total black carbon was estimated at +0.2 Wm^{-2} in the IPCC Third Assessment Report (Ramaswamy et al., 2001) and 0.55 Wm^{-2} in the IPCC Fourth Assessment Report (Forster et al., 2007).

A global mean radiative forcing estimation of ~0.02754 Wm^{-2} quantifies the contribution of fire to the Earth's system, in which forest fires show the most dramatic impact per area unit. Large extreme events can be detected in annual basis and show abrupt changes in shortwave albedo and its associated radiative forcing. Although the fire incidence in Africa is the highest with little inter-annual oscillations, the biggest changes in annual radiative forcing is caused by the extreme fire events in Australia, Europe and North America.

Anomalous fire events in continental Australia along with the boreal forests drive the global annual extremes of mean radiative forcing and show an excellent opportunity for future research efforts in that field.

Acknowledgements

The research leading to these results has received funding from the European Community's Seventh Framework Programme (FP7 2007-2013) under grant agreement n° 238366. For all our colleagues at LDRAG, thank you for your support. Dr Duarte Oom: SMA&D&N. Haifa & Dominik, Gerannis loves you.

References

Aragão, L. E. O. C. and Shimabukuro, Y. E.: The incidence of fire in Amazonian forests with implications for REDD, Science, 328.5983, 1275-1278, doi:10.1126/science.1186925, 2010.

Australian Government. http://www.bom.gov.au/climate/enso/enlist/ last access: 30 April 2014.

Boisier, J. P., de Noblet-Ducoudré, N. and Ciais, P.: Inferring past land use-induced changes in surface albedo from satellite observations: a useful tool to evaluate model simulations, Biogeosciences, 10(3), 1501–1516, doi:10.5194/bg-10-1501-2013, 2013.

Bond, T.C., Streets, D., Yarber, K.F., Nelson, S.M., Woo, J.-H., Klimont, Z:. A technology-based global inventory of black and organic carbon emissions from combustion. J. Geophys. Res. 109, 2004.

Bowman, D. M. J. S., Balch, J. K., Artaxo, P., Bond, W. J., Carlson, J. M., Cochrane, M. a, D'Antonio, C. M., Defries, R. S., Doyle, J. C., Harrison, S. P., Johnston, F. H., Keeley, J. E., Krawchuk, M. a, Kull, C. a, Marston, J. B., Moritz, M. a, Prentice, I. C., Roos, C. I., Scott, A. C., Swetnam, T. W., van der Werf, G. R. and Pyne, S. J.: Fire in the Earth system., Science, 324, 481-484, doi:10.1126/science.1163886, 2009.

Chubarova, N., Nezval', Y., Sviridenkov, I., Smirnov, a. and Slutsker, I.: Smoke aerosol and its radiative effects during extreme fire event over Central Russia in summer 2010, Atmos. Meas. Tech., 5(3), 557–568, doi:10.5194/amt-5-557-2012, 2012.

Chuvieco, E., Giglio, L. and Justice, C.: Global characterization of fire activity: toward defining fire regimes from Earth observation data, Glob. Chang. Biol., 14(7), 1488–1502, doi:10.1111/j.1365-2486.2008.01585.x, 2008.

Friedl, M. a., Sulla-Menashe, D., Tan, B., Schneider, A., Ramankutty, N., Sibley, A. and Huang, X.: MODIS Collection 5 global land cover: Algorithm refinements and characterization of new datasets, Remote Sens. Environ., 114(1), 168–182, doi:10.1016/j.rse.2009.08.016, 2010.

Forster, P., V. Ramaswamy, P. Artaxo, T. Berntsen, R. Betts, D.W. Fahey, J. Haywood, J. Lean, D.C. Lowe, G. Myhre, J. Nganga, R. Prinn, G. Raga, M. Schulz and R. Van Dorland, 2007: Changes in Atmospheric Constituents and in Radiative Forcing. In: Climate Change

2007: The Physical Science Basis. Contribution of Working Group I to the Fourth Assessment Report of the Intergovernmental Panel on Climate Change [Solomon, S., D. Qin, M. Manning, Z. Chen, M. Marquis, K.B. Averyt, M.Tignor and H.L. Miller (eds.)]. Cambridge University Press, Cambridge, United Kingdom and New York, NY, USA, 129-234, 2007.

Giglio, L., Loboda, T., Roy, D. P., Quayle, B. and Justice, C. O.: An active-fire based burned area mapping algorithm for the MODIS sensor, Remote Sens. Environ., 113(2), 408–420, doi:10.1016/j.rse.2008.10.006, 2009.

Govaerts, Y. M., Pereira, J.M., Pinty, B., and Mota, B.: Impact of fires on surface albedo dynamics over the African continent, J. Geophys. Res., 107, 4629, doi:10.1029/2002JD002388, 2002.

Gray, L. J., Beer, J., Geller, M., Haigh, J. D., Lockwood, M., Matthes, K., Cubasch, U., Fleitmann, D., Harrison, G., Hood, L., Luterbacher, J., Meehl, G. A., Shindell, D., van Geel, B. and White, W.: Solar Influences on Climate, Rev. Geophys., 48, RG4001, doi:10.1029/2009RG000282, 2010.

Holben, B.N., Smirnov, A., Eck, T.F., Slutsker, I., Abuhassan, N., Newcomb, W.W., Schafer, J.S., Tanre, D., Chatenet, B., Lavenu, F.: An emerging ground-based aerosol climatology - Aerosol optical depth from AERONET. J. Geophys. Res. 106, 12067– 12097, 2001.

Jin, Y., Randerson, J. T., Goetz, S. J., Beck, P. S. a., Loranty, M. M. and Goulden, M. L.: The influence of burn severity on postfire vegetation recovery and albedo change during early succession in North American boreal forests, J. Geophys. Res., 117(G1), G01036, doi:10.1029/2011JG001886, 2012.

Jin, Y., Randerson, J. T., Goulden, M. L. and Goetz, S. J.: Post-fire changes in net shortwave radiation along a latitudinal gradient in boreal North America, Geophys. Res. Lett., 39(13), doi:10.1029/2012GL051790, 2012.

Jin, Y., Roy, D. P.: Fire-induced albedo change and its radiative forcing at the surface in northern Australia, Geophys. Res. Lett., 32(13), L13401, doi:10.1029/2005GL022822, 2005.

Ju, J., Roy, D. P., Shuai, Y. and Schaaf, C.: Development of an approach for generation of temporally complete daily nadir MODIS reflectance time series, Remote Sens. Environ., 114(1), 1–20, doi:10.1016/j.rse.2009.05.022, 2010.

Kalnay, E., Kanamitsu, M., Kistler, R., Collins, W., Deaven, D., Gandin, L., Iredell, M., Saha, S., White, G., Woollen, J., Zhu, Y., Leetmaa, A., Reynolds, R., Chelliah, M., Ebisuzaki, W., Higgins, W., Janowiak, J., Mo, K. C., Ropelewski, C., Wang, J., Jenne, R. and Joseph, D.: The NCEP/NCAR 40-Year Reanalysis Project, B. Am. Meteorol. Soc., 77, 437–471, 1996.

Lewis, S.L., Brando, P.M., Phillips, O.L., van der Heijden, G.M.F., and Nepstad, D.: The 2010 Amazon drought. Science, 331, 554, doi:10.1126/science.1200807, 2011.

Liang, S.: Narrowband to broadband conversions of land surface albedo I Algorithms, Remote Sens. Environ., 76(2000), 213–238, 2001.

Lucht, W. and Lewis, P.: Theoretical noise sensitivity of BRDF and albedo retrieval from the EOS-MODIS and MISR sensors with respect to angular sampling, Int. J. Remote Sens., 21(1), 81–98, doi:10.1080/014311600211000, 2000.

Lucht, W., Schaaf, C. B. and Strahler, a. H.: An algorithm for the retrieval of albedo from space using semiempirical BRDF models, IEEE Trans. Geosci. Remote Sens., 38(2), 977–998, doi:10.1109/36.841980, 2000.

MCD64A1 burned area product. ftp://fuoco.geog.umd.edu/db/MCD64A1/ last access: 24 April 2014.

NCEP/NCAR dswrf at the surface. ftp://ftp.cdc.noaa.gov/Datasets/ncep.reanalysis.derived/surface_gauss/dswrf.sfc.mon.mean.nc last access: 24 April 2014.

Pereira, J. M.: A comparative evaluation of NOAA/AVHRR vegetation indexes for burned surface detection and mapping, IEEE Trans. Geosci. Remote Sens., 37(1), 217–226, doi:10.1109/36.739156, 1999.

Prentice, I. C., Baines, P. G., Scholze, M., and Wooster, M. J.: Fundamentals of climate change science, in: Understanding the Earth System: Global Change Science for Application, edited by: CornellS. E., Prentice, I. C., House, J. I., and Downy, C. J., Cambridge University Press, 39–71, 2012.

Ramaswamy, V., Boucher, O., Haigh, J. D., Hauglustaine, D., Haywood, J., Myhre, G., Nakajima, T., Shi, G. Y., and Solomon, S.: Radiative Forcing of Climate Change, in: Climate Change 2001: The Scientific Basis. Contribution of Working Group I to the Third Assessment Report of the Intergovernmental Panel on Climate Change, edited by: Houghton, J. T., Ding,

Y., Griggs, D. J., Noguer, M., van der Linden, P. J., Dai, X., Maskell, K., and Johnson, C. A., Cambridge University Press, Cambridge, UK and New York, NY, USA, 349–416, 2001.

Schaaf, C. B., Gao, F., Strahler, A. H., Lucht, W., Li, X., Tsang, T., Strugnell, N. C., Zhange, X., Jin, Y., Muller, J. P., Lewis, P., Barnsley, M., Hobson, P., Disney, M., Roberts, G., Dunderdale, M., Doll, C., d'Entremont, R. P., Hu, B., Liang, S., Privett, J. L., and Roy, D.: First operational BRDF, albedo nadir reflectance products from MODIS, Rem. Sens. Environ., 83, 135–148, 2002.

Sheng, Y., Smith, L. C., MacDonald, G. M., Kremenetski, K. V., Frey, K. E., Velichko, A. a., Lee, M., Beilman, D. W. and Dubinin, P.: A high-resolution GIS-based inventory of the west Siberian peat carbon pool, Global Biogeochem. Cycles, 18, 3, GB3004, doi:10.1029/2003GB002190, 2004.

Shvidenko, A. Z., Shchepashchenko, D. G., Vaganov, E. A., Sukhinin, A. I., Maksyutov, S. S., McCallum, I., and Lakyda, I. P.: Impact of wildfire in Russia between 1998–2010 on ecosystems and the global carbon budget, Dokl. Earth Sci., 441, 1678-1682, doi:10.1134/S1028334X11120075, 2011.

Stroppiana, D., Pinnock, S., Pereira, J. M. and Grégoire, J.-M.: Radiometric analysis of SPOT-VEGETATION images for burnt area detection in Northern Australia, Remote Sens. Environ., 82(1), 21–37, doi:10.1016/S0034-4257(02)00021-4, 2002.

Turquety, S., Logan, J. a., Jacob, D. J., Hudman, R. C., Leung, F. Y., Heald, C. L., Yantosca, R. M., Wu, S., Emmons, L. K., Edwards, D. P. and Sachse, G. W.: Inventory of boreal fire emissions for North America in 2004: Importance of peat burning and pyroconvective injection, J. Geophys. Res., 112(D12), D12S03, doi:10.1029/2006JD007281, 2007.

Van der Werf, G. R., Randerson, J. T., Giglio, L., Collatz, G. J., Mu, M., Kasibhatla, P. S., Morton, D. C., DeFries, R. S., Jin, Y. and van Leeuwen, T. T.: Global fire emissions and the contribution of deforestation, savanna, forest, agricultural, and peat fires (1997–2009), Atmos. Chem. Phys., 10(23), 11707–11735, doi:10.5194/acp-10-11707-2010, 2010.

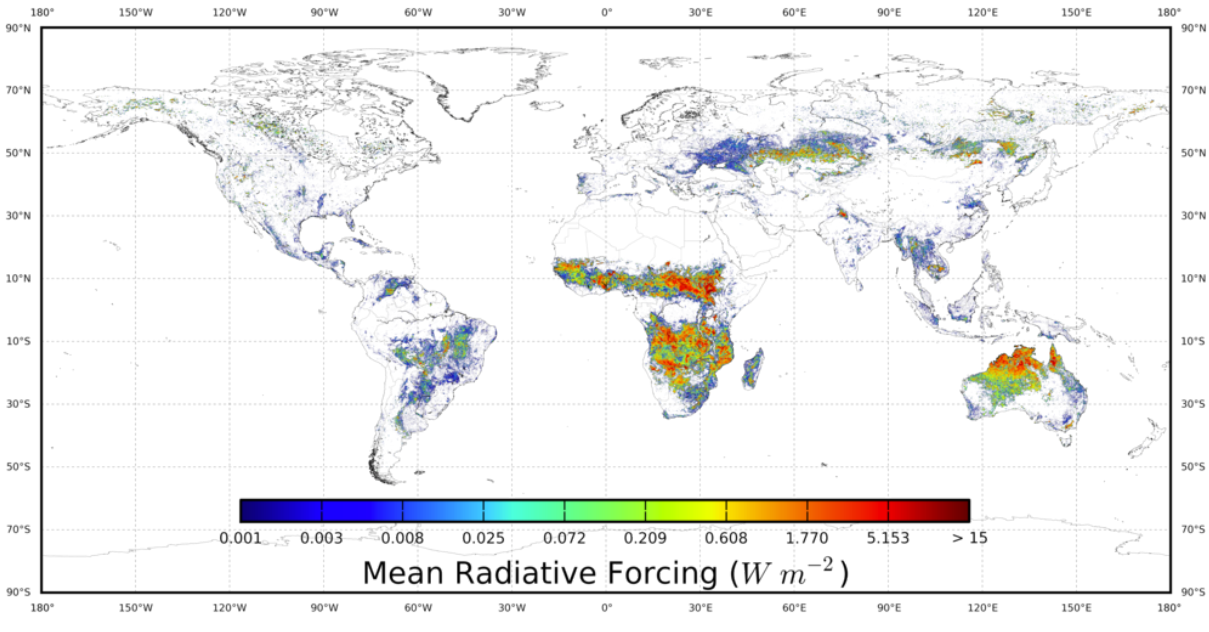

Figure 1. Global mean radiative forcing caused by "instantaneous" shortwave albedo changes on areas affected by fires during 2002-2012. The values were normalized using a logarithmic scale.

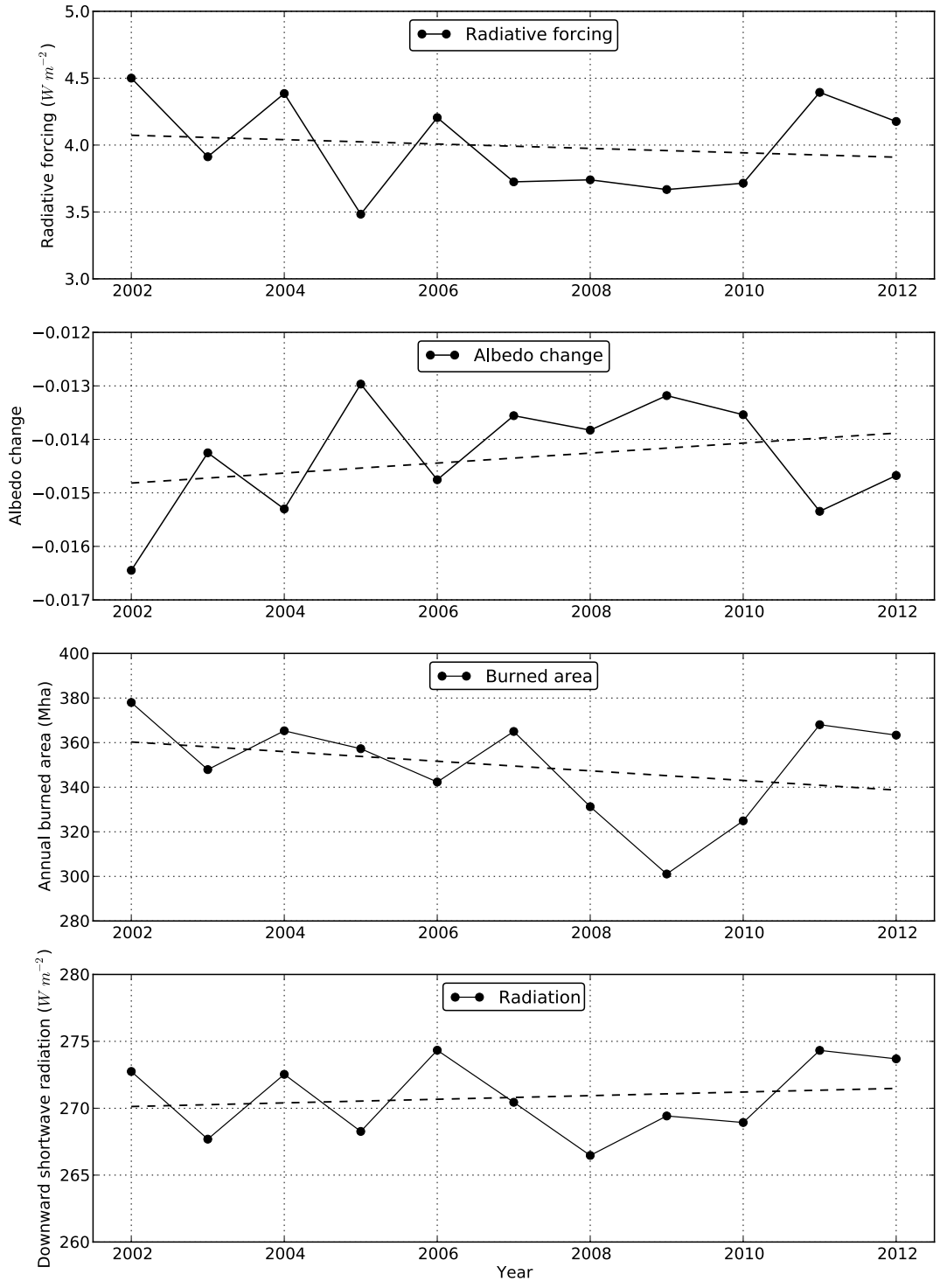

Figure 2. Temporal changes of the annual global radiative forcing induce by fires and albedo change spanning from 2002 to 2012. Bottom plots show the total annual burned area and the downward shortwave radiation fluxes at the surface. The dashed lines depict linear trends, where changes of rate per year are, for radiative forcing: -0.016Wm^{-2}, albedo change: 9.33e-

05, burned area: -2.15Mha and downward shortwave incoming radiation: 0.14 Wm^{-2}.~~Figure 2. Temporal changes of the annual global radiative forcing induce by fires (blue line) and albedo change (in red) spanning from 2002 to 2012. Bottom plots show the total annual burned area and the downward shortwave radiation fluxes at the surface. The spatial variations (one standard deviation) in radiative forcing, albedo change and shortwave radiation are plotted as vertical bars. The dashed lines depict linear trends.~~

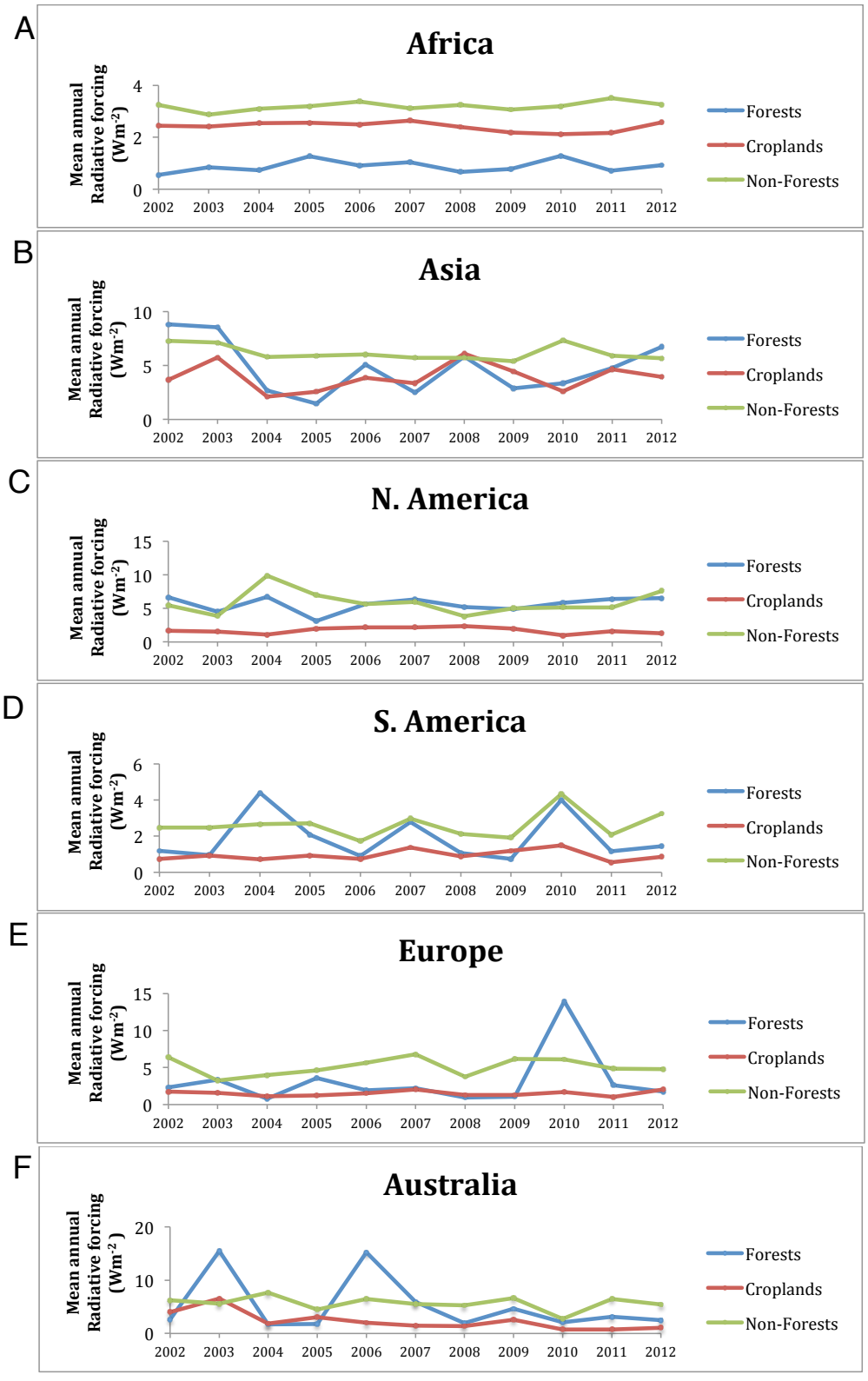

Figure 3. The mean annual radiative forcing per land cover and continent (A-F).

A

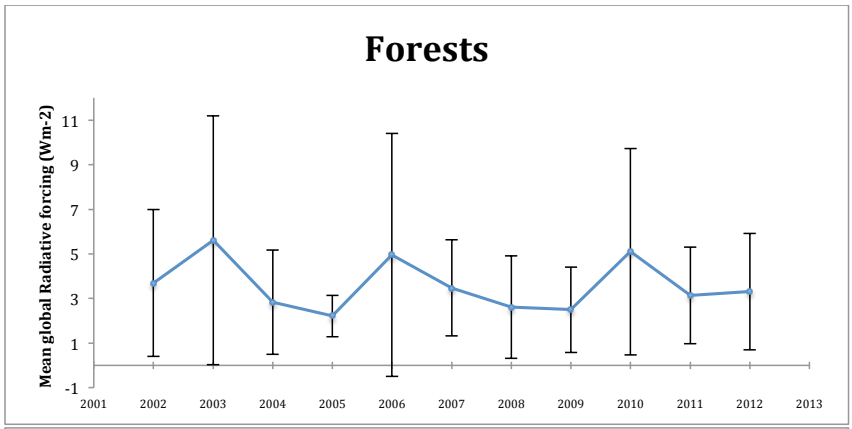

B

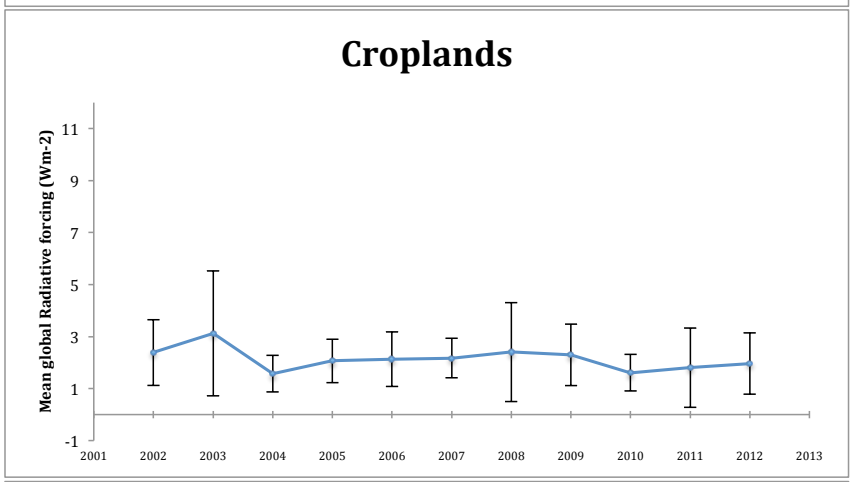

C

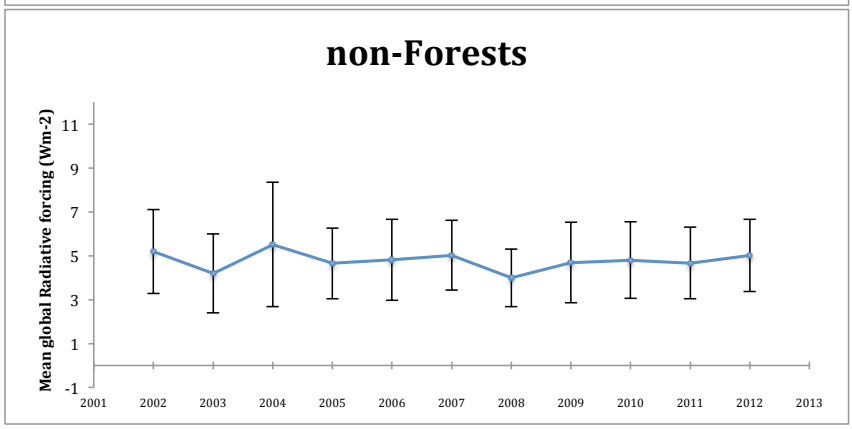

Figure 4. The mean annual radiative forcing per land cover (A-C) in Wm^{-2}.

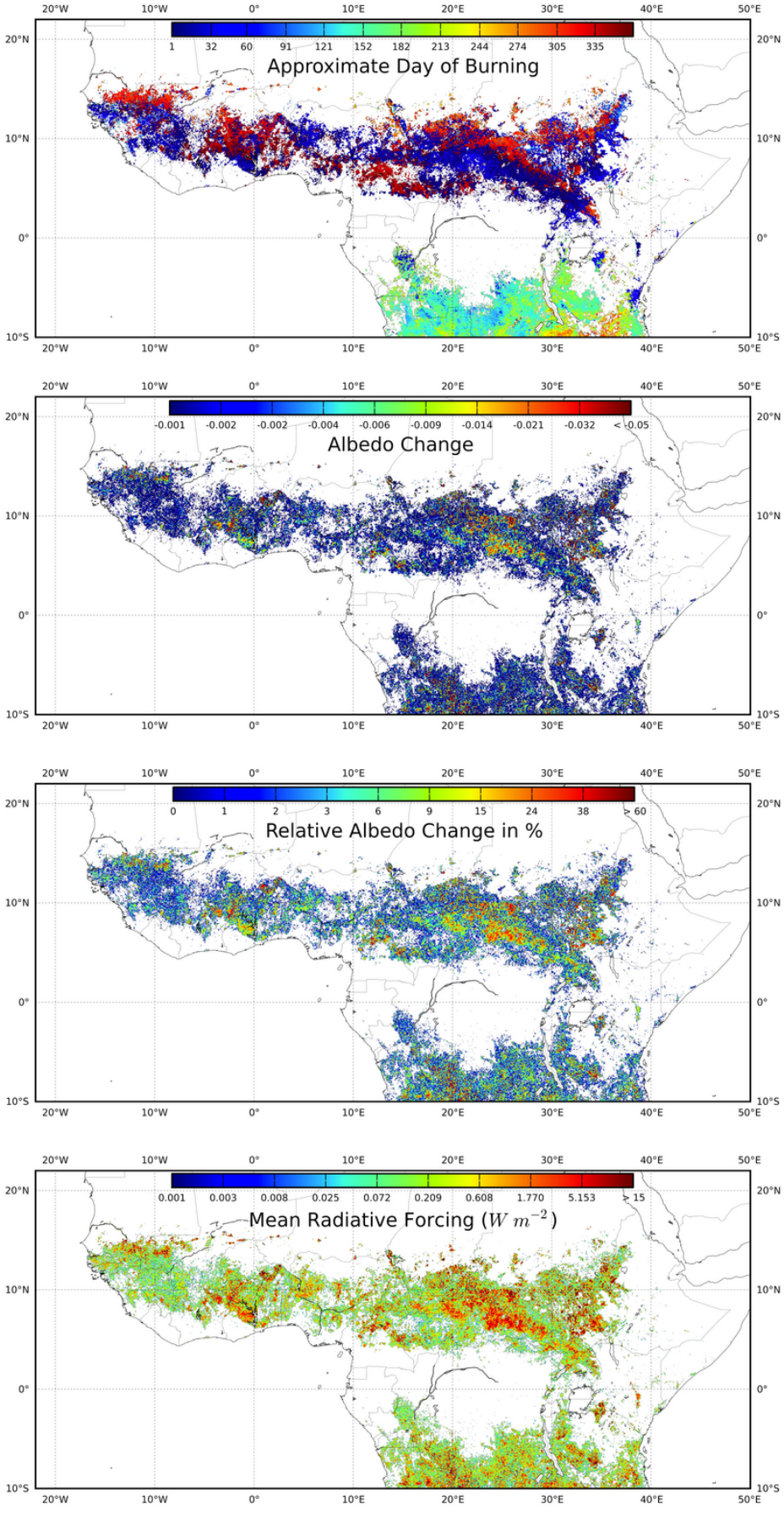
Approximate Day of Burning
1 32 60 91 121 152 182 213 244 274 305 335
Albedo Change
-0.001 -0.002 -0.002 -0.004 -0.006 -0.009 -0.014 -0.021 -0.032 < -0.05
Relative Albedo Change in %
0 1 2 3 6 9 15 24 38 > 60
Mean Radiative Forcing ($W\ m^{-2}$)
0.001 0.003 0.008 0.025 0.072 0.209 0.608 1.770 5.153 > 15
20°W 10°W 0° 10°E 20°E 30°E 40°E 50°E
20°N 10°N 0° 10°S

1

Figure 5. The approximate day of burning; the "instantaneous" shortwave albedo change in areas affected by fire; the relative change in albedo in % and the associated radiative forcing in Wm^{-2} is shown for the Sahel during 2003.

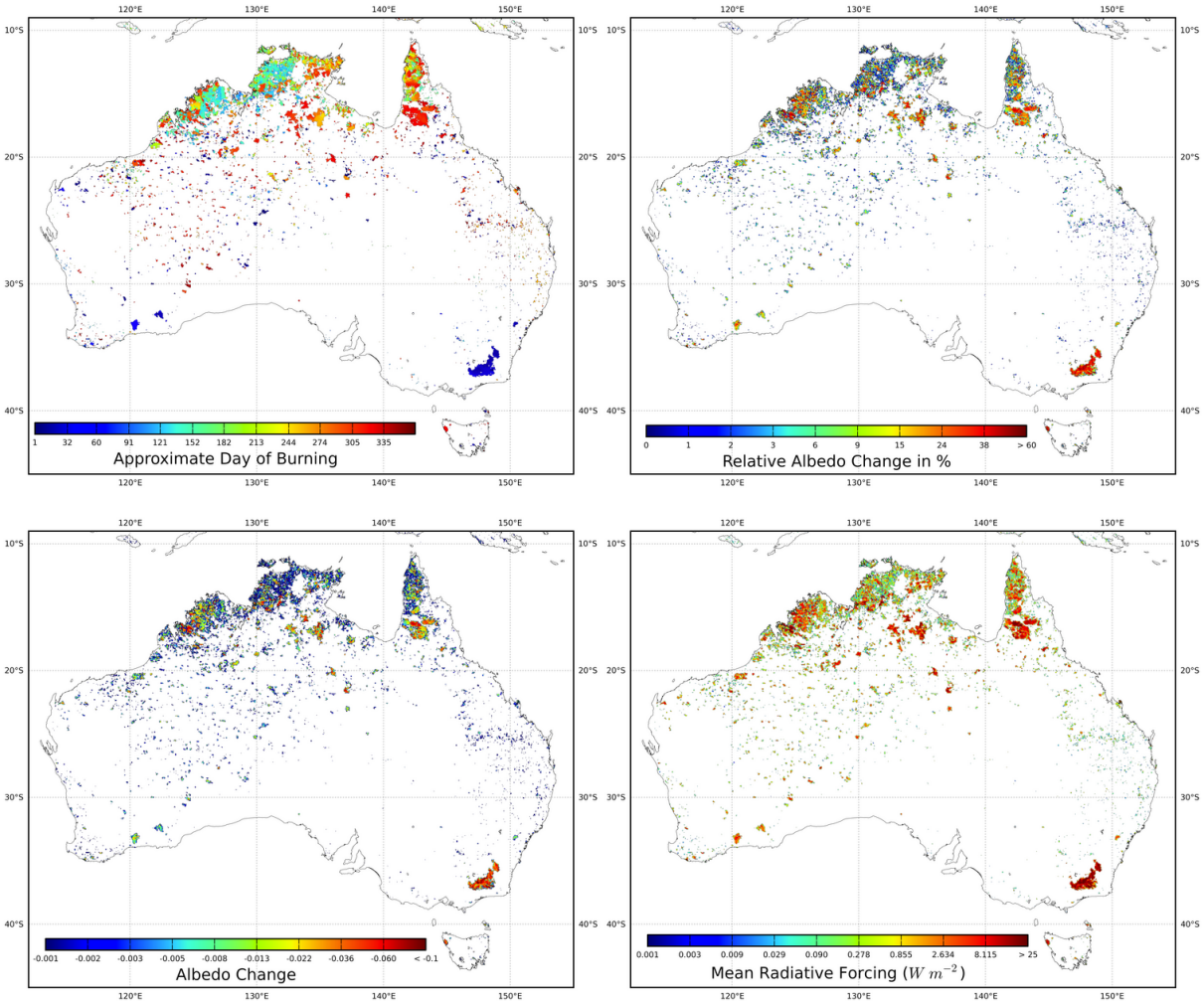

Figure 6. The approximate day of burning; the "instantaneous" shortwave albedo change in areas affected by fire; the relative albedo change in % and the associated radiative forcing in Wm^{-2} is shown for Australia during 2003.

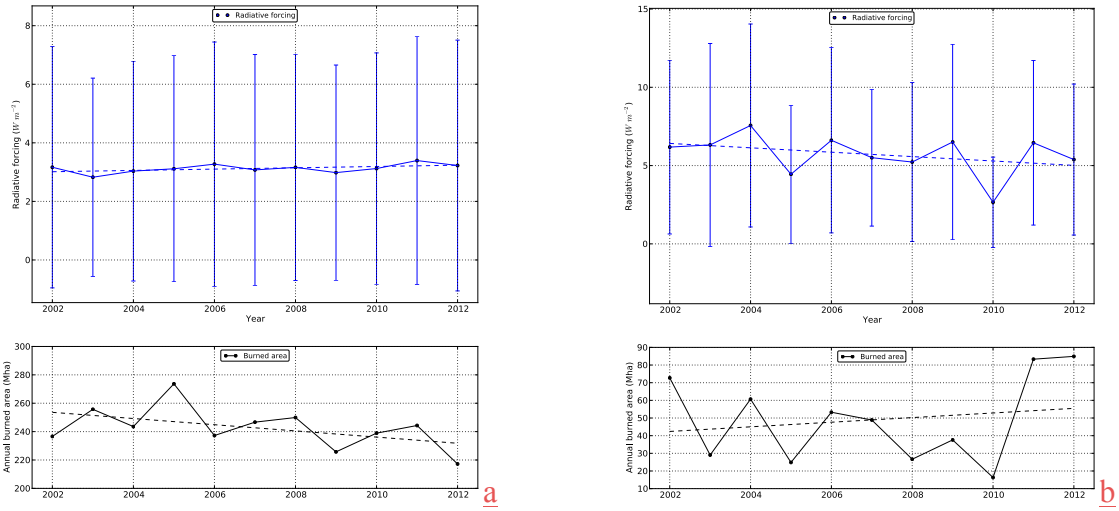

Figure 7. Temporal evolution of the radiative forcing and burned areas. Panel a) shows the profiles for Africa, panel b) for Australia.

1

2